

Orientation-dependent x-ray absorption fine structure of ZnO nanorods

S.-W. Han^{a)} and H.-J. Yoo

Division of Science Education, Chonbuk National University, Jeonju 561-756, Korea

Sung Jin An, Jinkyong Yoo, and Gyu-Chul Yi

National CRI Center for Semiconductor Nanorods and the Department of Materials Science and Engineering, Pohang University of Science and Technology (POSTECH), Pohang 790-784, Korea

(Received 26 July 2004; accepted 16 November 2004; published online 6 January 2005)

The local structure of two samples of vertically well-aligned ZnO nanorods with average diameters of 13 and 37 nm were studied using orientation-dependent x-ray absorption fine structure (XAFS) at the Zn *K* edge. The aligned ZnO nanorod samples were fabricated on sapphire (0001) substrates with a catalyst-free metalorganic vapor-phase epitaxy method. The XAFS measurements showed that both nanorod samples have a well-ordered wurtzite structure and that no vacancy was observed at either site of zinc or oxygen atoms. However, we found that in both samples the lattice constants of *a* and *b* were shrunken by ~ 0.04 Å while *c* was elongated by ~ 0.1 Å, compared with those of their bulk counterparts. Furthermore, there was a substantial amount of disorder in the bond length of the only Zn–O pairs located near the *ab* plane. This may suggest that the terminating atoms at the boundaries of the nanorods are oxygen atoms. © 2005 American Institute of Physics. [DOI: 10.1063/1.1851616]

One-dimensional (1D) nanocrystalline semiconductors including nanorods, nanotubes and nanowires have attracted considerable attention for their practical applications to nanometer-scale electronics and photonics as well as for fundamental academic research.^{1,2} The physical properties of 1D nanomaterials are dependent on orientations because their size and surface effects also depend on the orientations. The orientation-dependent quantum confinement effect was observed from ZnO nanorods and ZnO/ZnMgO nanorod heterostructures.³ For better understanding of the physical properties of 1D nanomaterials, the study of orientation-dependent structural properties is necessary because structural transitions including distortions and disorders as well as surface and size effects contribute to the determination of the properties.⁴ However, no study of the local structural properties of a 1D nanomaterial has been reported. The diffraction technique is a powerful tool to investigate the structures of crystalline materials but not of nanomaterials. Regular x-ray absorption fine structure (XAFS) can describe the average bond lengths and the distributions of the bond lengths from a probe atom.⁵ However, regular XAFS cannot separate the structural properties dependent on crystalline orientations, as like atoms are located at similar distances.

In this letter, we first report the structural properties and terminating atoms of 1D ZnO nanorods. We employed the orientation-dependent XAFS which can determine the angles and distances of bonds,⁶ to discern the structural properties in the *ab* plane and along the *c* axis of ZnO nanorods with diameters of 13 and 37 nm. Note that the quantum confinement effect was observed from ZnO nanorods with a diameter of less than 20 nm.³ For ZnO with a wurtzite structure, Zn atoms have four oxygen atoms and 12 zinc atoms as the first and second neighboring atoms, respectively, in all directions. Two independent XAFS measurements from the ZnO nanorods were made with the x-ray polarizations parallel and

perpendicular to the *c* axis. Both sets of XAFS data were simultaneously fitted with the same parameters and the orientation-dependent structural distortions of the nanorods were obtained and compared with their ZnO bulk counterparts.

Vertically well-aligned ZnO nanorods were fabricated on Al₂O₃(0001) substrates at 500 and 800 °C for 1 h using catalyst-free metalorganic vapor-phase epitaxy. The average diameters of the rods grown at 500 and 800 °C were 37 ± 3 and 13 ± 5 nm, respectively and the mean length along *c* axis was about 1 μm.² X-ray diffraction and high resolution transmission electron microscopy (TEM) measurements showed that the nanorods were well-ordered single crystals and vertically well-aligned rods.^{2,3} Fluorescence XAFS data at the Zn *K* edge (9659 eV) were collected by selecting the incident x-ray energy with a 25% detuned Si(111) double monochromator. Figure 1 shows the normalized x-ray absorption coefficient from the ZnO nanorods near the Zn *K* edge as a function of the incident x-ray energy, measured at

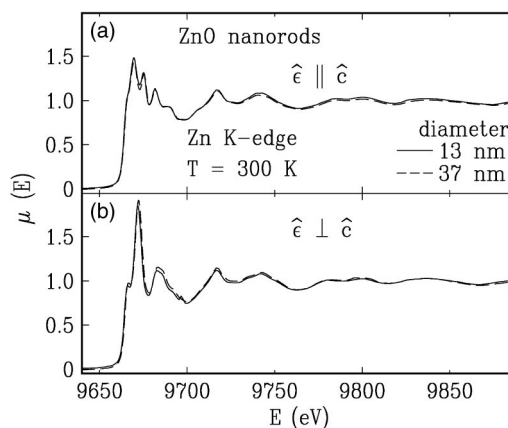


FIG. 1. Normalized x-ray absorption coefficient from ZnO nanorods as a function of incident x-ray energy at the Zn *K* edge with the geometry of the $\hat{\epsilon}$ axis aligned, (a) parallel and (b) perpendicular, to the electric field vector of the x rays.

^{a)} Author to whom correspondence should be addressed; electronic mail: swhan@chonbuk.ac.kr

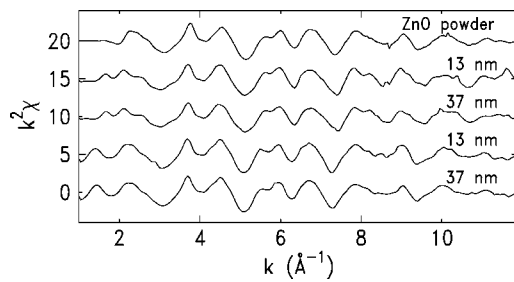


FIG. 2. XAFS ($k^2\chi$) from ZnO powder (top) and from the aligned ZnO nanorods with diameters of 13 and 37 nm for $\hat{\epsilon}\parallel\hat{c}$ (2nd and 3rd) and $\hat{\epsilon}\perp\hat{c}$ (4th and 5th), as a function of the photoelectron wave vector k .

room temperature for the two orientations. At Zn K edge, the x-ray self-absorption of the ZnO nanorods with about 1 μm length is negligible. The near edge structures from the rods clearly show the dependence of the crystal orientations and are comparable with Chiou's study.⁷

The local structural properties around a probe atom can be obtained by looking at the fine structure above the absorption edge.⁵ The orientation-dependent XAFS data were analyzed with the UWXAFS package⁸ using standard procedures⁶ and photoelectron backscattering functions calculated with the FEFF8 code.⁹ After the atomic background absorption μ_0 was determined using AUTOBK (part of the UWXAFS package), the XAFS function, $\chi = \mu(E)/\mu_0(E) - 1$, was obtained. Figure 2 shows the XAFS from ZnO powder and nanorods at the Zn K edge for $\hat{\epsilon}\parallel\hat{c}$ and $\hat{\epsilon}\perp\hat{c}$, as a function of the photoelectron wave vector, $k = \sqrt{2m_e(E - E_0)}/\hbar$, where m_e is the electron rest mass, E is the incident photon energy and E_0 is the edge energy. To minimize uncertainties only the XAFS data in the k range of 2.5–10.5 \AA^{-1} were used for further analysis.

The XAFS data were Fourier transformed to r space and fit to the theoretical XAFS calculations,⁹ as shown in Fig. 3. The fits included single- and multi-scattering paths and 95% polarization of the incident x ray was taken into account in the data analysis. The dotted lines in Fig. 3 show the magnitudes of the Fourier transformed XAFS data from ZnO powder, and nanorods with a diameter of 13 nm. Note that the peaks are shifted by about 0.5 \AA on the \tilde{r} axis from their true bond lengths due to the phase shift of the backscattered photoelectrons. Detailed fits are therefore necessary to obtain quantitative information. For the fit of the ZnO powder data, we constructed a fully occupied model of a wurtzite structure, the results of which are summarized in Table I. From the fit, we found the lattice constants of $a, b = 3.246(13)$ \AA and $c = 5.206(12)$ \AA , which agree well with the results of previous studies of bulk ZnO.^{10,11} The Debye–Waller factors

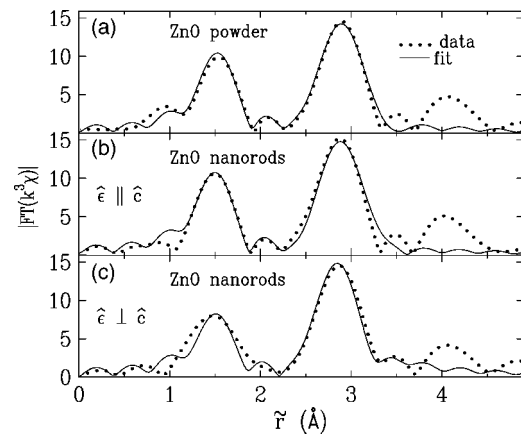


FIG. 3. Magnitude of Fourier transformed XAFS, from (a) ZnO powder and ZnO nanorods with an average diameter of 13 nm for (b) $\hat{\epsilon}\parallel\hat{c}$ and (c) $\hat{\epsilon}\perp\hat{c}$, as a function of the distance from a Zn atom. For the Fourier transformation, a Hanning window with a windowsill width of 0.5 \AA^{-1} was used. Data in the range of $\tilde{r} = 1.2\text{--}3.5$ \AA were used for the fit.

(σ^2 , including thermal vibration and static disorder) of Zn–O and Zn–Zn pairs of the ZnO powder were 0.003(1) \AA^2 and 0.008(2) \AA^2 , respectively, which again are comparable with those of previous reports.^{10,11}

To accurately determine the orientation-dependent structural properties with the XAFS data of the nanorods, the two sets of XAFS data in Figs. 3(b) $\hat{\epsilon}\parallel\hat{c}$ and 3(c) $\hat{\epsilon}\perp\hat{c}$ were simultaneously fitted. The results of the best fit are given in Table I. From a probe Zn atom, the distance of O(1) located just above the Zn atom along the c axis was ~ 0.05 \AA longer while the distance of three O(2)s located about 19° off from the Zn ab plane was about 0.025 \AA shorter, compared with those bond lengths of the bulk counterpart. These results were similar to the bond length distortions of the Zn–Zn(1) pairs located $\sim 55^\circ$ off from the ab plane and the Zn–Zn(2) pairs located in the ab plane, as shown in Table I. Based on these fits, the lattice constants were estimated to be $a = b \approx 3.216(3.195)$ \AA and $c \approx 5.305(5.307)$ \AA for the ZnO nanorods with a diameter of 13(37) nm. A cumulant analysis to search for an anharmonic pair-distance distribution was, however, inconclusive. We concluded that the lattice constants of ZnO nanorods, a and b , were shrunken by about 0.04 \AA , while c was elongated by 0.1 \AA , compared with those of the bulk counterpart.

The relative mean squared disorder of all pairs except the Zn–O(2) pairs in both nanorod samples was very comparable with those of the bulk, implying that there was no extra disorder in the bond lengths of the nanorods. The ratio of atomic pairs in the boundary to the total number of the

TABLE I. Coordination number (N), bond length (d) and Debye–Waller factor (σ^2) of ZnO bulk and nanorods were determined with simultaneous fits of orientation-dependent XAFS data measured at the Zn K edge. S_0^2 of 0.95 was determined from the fit of the powder data and fixed for the fits of the nanorod data. For the model calculations, a fully occupied wurtzite structure (space group: $p63m$) with $a, b = 3.245$ \AA , $c = 5.205$ \AA and the crystalline symmetry z of oxygen = 0.366 was used.

Specimen	N	Zn–O(1)		Zn–O(2)		Zn–Zn(1)		Zn–Zn(2)			
		$d(\text{\AA})$	$\sigma^2(\text{\AA}^2)$	N	$d(\text{\AA})$	$\sigma^2(\text{\AA}^2)$	N	$d(\text{\AA})$	$\sigma^2(\text{\AA}^2)$		
Model	1	1.9050		3	1.9991	6	3.2067		6	3.2450	
Powder	1	1.903(9)	0.003(1)	3	1.981(18)	6	3.206(10)	0.008(2)	6	3.246(13)	0.008(2)
Nanorods (13 nm)	1.0(1)	1.947(8)	0.0037(7)	3.1(4)	1.965(12)	6.2(3)	3.236(4)	0.0084(15)	6.2(6)	3.214(6)	0.0087(16)
Nanorods (37 nm)	1.0(1)	1.966(6)	0.0028(8)	2.7(3)	1.950(9)	6.0(2)	3.231(4)	0.0090(14)	5.7(5)	3.195(6)	0.0089(15)

pairs in a nanorod can be simply estimated with $(\pi R^2 - \pi(R-D)^2)/\pi R^2$, where R is the radius of the rods and D is the distance from the boundary.¹² Assuming that only the first and second atomic layers ($D \approx 0.65$ nm) from the boundary were effectively affected by the incomplete bonds at the boundary, about 19% of the Zn–Zn pairs in nanorods with a diameter of 13 nm had an extra disorder. However, from the orientation dependent XAFS measurements, neither extra disorder nor vacancy at the Zn sites in all directions was observed, compared with the bulk counterpart. This strongly suggests that the Zn atoms are well ordered in the *ab* plane even near the boundary, as well as along the *c* axis, and that the terminating atoms at the boundary are oxygen atoms. As the O(2)s are the terminating atoms at the boundary, the ratio of the Zn–O(2) pairs located near the boundary to the total Zn–O(2) pairs is inverse to the diameter of the rods. Therefore, more disorders will exist in the bond length of the Zn–O(2) pairs for the nanorods with a smaller diameter. The XAFS data analysis of the Zn–O(2) pairs was consistent with this scenario. Our observations of the terminating-oxygen atoms and the well-ordered structure at the boundary of the ZnO nanorods are in agreement with the high resolution TEM and x-ray diffraction measurements of vertically aligned nanorods,¹³ but not with Wu *et al.* who reported a large amount of disorder and a vacancy rate of about 20% of the Zn–Zn pairs in a ZnO film.¹¹ However, we cannot eliminate the possibility of O–H bonds at the boundary due to the lack of XAFS sensitivity to hydrogen atoms.

In conclusion, the orientation-dependent XAFS measurements showed that nanorods with diameters of 13 and 37 nm have a well-ordered wurtzite structure even at the boundary of the rods, but that the lattices are shrunken in the *ab* plane and expanded along the *c* axis, compared with their bulk counterparts. The local structural properties of the two nanorods were very similar except the σ^2 of Zn–O(2) pairs due to the terminating- O(2) (or O–H) atoms at the boundary. These results imply that the quantum confinement observed

from the ZnO nanorods was due to the size effect.

Work at Chonbuk National University was done under the auspices of the research fund of the Chonbuk National University and the Koran MOST through Proton Accelerator User Program (No. M202AK010021-04A1101-02110) of Proton Engineering R&D Project from the Nuclear R&D Program and the 21th Century Frontier R&D Program, and work at POSTECH was supported by the National Creative Research Initiative Project of the Ministry of Science and Technology. The XAFS data were collected at the 3C1 beam-line of the Pohang Light Source, Korea, a facility which is partially supported by MOST and POSCO.

¹X. Duan, Y. Hunag, Y. Cui, J. Wang, and C. M. Lieber, *Nature (London)* **409**, 66 (2001); M. H. Huang, S. Mao, H. Feick, H. Yang, Y. Wu, H. Kind, E. Weber, R. Russo, and P. Yang, *Science* **292**, 1897 (2001).

²W. I. Park, D. H. Kim, S.-W. Jung, and G.-C. Yi, *Appl. Phys. Lett.* **80**, 4232 (2002).

³W. I. Park, Y. H. Jun, S. W. Jung, and Gyu-Chul Yi, *Appl. Phys. Lett.* **82**, 964 (2003); W. I. Park, Gyu-Chul Yi, Miyoung Kim, and Stephen J. Pennycook, *Adv. Mater. (Weinheim, Ger.)* **15**, 1841 (2002).

⁴S.-W. Han, C. H. Booth, E. D. Bauer, P. H. Huang, Y. Y. Chen, and J. M. Lawrence, *J. Magn. Magn. Mater.* **272–276**, e101 (2004); S.-W. Han, *Jpn. J. Appl. Phys., Part 1* **42**, 6303 (2003).

⁵E. A. Stern, *Phys. Rev. B* **10**, 3027 (1974); J. J. Rehr and R. C. Albers, *ibid.* **41**, 8139 (1999).

⁶S.-W. Han, E. A. Stern, D. Hankel, and A. R. Moodenbaugh, *Phys. Rev. B* **66**, 094101 (2002).

⁷J. W. Chiou, J. C. Jan, H. M. Tsai, C. W. Bao, W. F. Pong, M.-H. Tsai, I.-H. Hong, R. Klauser, J. F. Lee, J. J. Wu, and S. C. Liu, *Appl. Phys. Lett.* **84**, 3462 (2004).

⁸E. A. Stern, M. Newville, B. Ravel, Y. Yacoby, and D. Haskel, *Physica B* **208,209**, 117 (1995).

⁹A. L. Ankudinov, B. Ravel, J. J. Rehr, and S. D. Conradson, *Phys. Rev. B* **58**, 7565 (1998).

¹⁰N. H. Tran, A. J. Hartmann, and R. N. Lamb, *J. Phys. Chem. B* **103**, 4264 (1999).

¹¹Z. Wu, Y. Zhou, and X. Zhang, *Appl. Phys. Lett.* **84**, 4442 (2004).

¹²R. W. Siegel, *Annu. Rev. Mater. Sci.* **21**, 559 (1991).

¹³S. J. An, W. Il Park, G.-C. Yi, Y.-J. Kim, H.-B. Kang, and M. Kim, *Appl. Phys. Lett.* **84**, 3612 (2004).